REDUCED CEMENTITIOUS MATERIAL IN OPTIMIZED CONCRETE MIXTURES: ANNUAL CELL PERFORMANCE REPORT

Contract Number: (C) 1003320 (WO) 3

Task 3: Analysis to Determine the Early-Age Characteristics of Concrete Paving Mixes with Lower Cementitious Content

Principal Investigator
Peter Taylor
Director
National Concrete Pavement Technology Center, Iowa State University

Co-Principal Investigator
Seyedhamed Sadati
Assistant Scientist IV
National Concrete Pavement Technology Center, Iowa State University

Performing Organization
National Concrete Pavement Technology Center
Iowa State University
2711 South Loop Drive, Suite 4700
Ames, IA 50010-8664
Phone: 515-294-8103 / Fax: 515-294-0467
www.cptechcenter.org

Sponsored by
Federal Highway Administration
Minnesota Department of Transportation
National Road Research Alliance Transportation Pooled Fund

Lead State Representative
Bernard Izevbekhai
Minnesota Department of Transportation
Office of Materials and Road Research, Mail Stop 645
1400 Gervais Avenue, Maplewood, Minnesota 55109
Phone: 651-366-5454
E-Mail: bernard.izevbekhai@state.mn.us

Table of Contents

LIST OF FIGURES

LIST OF TABLES

ACKNOWLEDGMENTS

The research team would like to express their gratitude to the Minnesota Department of Transportation (MnDOT) for sponsoring this research and the National Road Research Alliance (NRRA) for supporting this work.

INTRODUCTION

The present document addresses the work planned under Task 3 of the research proposal. The goal is to evaluate the early-age characteristics of concrete paving mixtures with reduced cementitious material content, intended to understand the potential placement issues and other material-related problems that can affect the performance of pavements cast with such mixtures.

Optimized concrete mixtures with reduced cementitious materials content were employed for construction of two test cells at MnROAD facility. Two concrete paving mixtures with “low” cementitious content, i.e., 500 lb/yd^3, and “lower” cementitious content, i.e., 470 lb/yd^3, were used at two identical (except for concrete mix) cells 138 and 238, respectively. Each cell is about 260 feet long.

Data obtained from relevant field and laboratory tests on fresh and hardened concrete samples were analyzed. Moreover, the data from in-situ tests conducted on pavement sections along with the observations recorded during the in-situ inspections were employed. Data presented in this report is intended to identify lower limits on cementitious materials content that mitigate placement and strength gain issues during construction.

PROJECT INFORMATION

The present project investigates the performance of two test cells (138 and 238) constructed with optimized concrete mixtures at MnROAD pavement research facility. Located in Albertville, 40 miles Northwest of Saint Paul Minnesota, the MnROAD research facility consists of two distinct segments of roadway: the Mainline (ML) and the Low Volume Road (LVR). MnROAD was built in 1993, comprising 23 original test cells at the time. As at 2016, there were a total of 69 test cells between the Mainline and LVR. A different pavement type and/or design is used in construction of each of these cells.

The Mainline is a 3.5 mile, 2-lane interstate highway that carries live traffic diverted from Westbound Interstate 94 while the LVR is a 2-lane wide closed loop with 24 test cells (in 2016) with a total length of 2.5 miles. The traffic on the LVR is restricted to a single 18-wheel, 5-axle tractor with trailer that is intended to simulate the traffic conditions on rural roads. Operation of this vehicle is performed by the MnROAD staff and according to a controlled schedule that includes 80 laps per day on the inside lane only. The outside lane is subjected to environmental loading only, except for the minimal loading from lightweight test vehicles. This restriction is intended to demonstrate the pavement response due to environmental effects versus loading effects.

The low cementitious test cells 138 and 238 are contiguously located on the LVR as presented in Figure 1. A concrete mixture with 500 lb/yd^3 of cementitious materials was used for building cell 138 and designated as the low cementitious mixture, while another similar mixture proportioned with 470 lb/yd^3 of cementitious materials content was used for cell 238 and designated as the lower cementitious mixture in this report. Data obtained from these two cells were compared to those gathered from testing the cell 524 proportioned with 570 lb/yd^3 of cementitious materials that serves as the reference cell in this study.

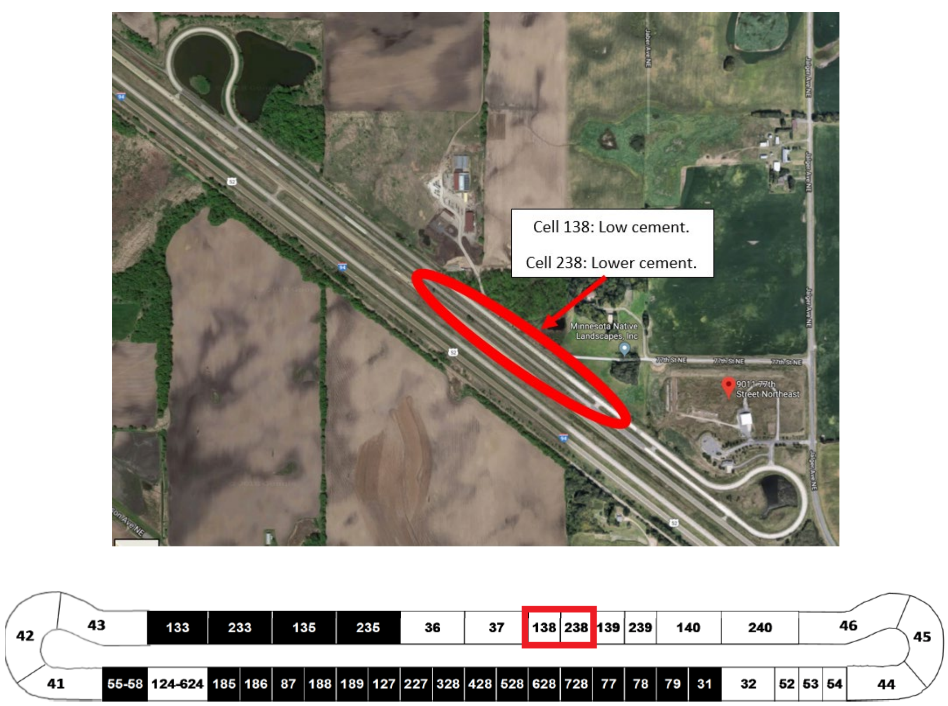

Figure 1- Aerial photo (top) and schematic view (bot.) of the investigated cells

Concrete placement, sampling, and testing took place on July 14, 2017. The construction activities, design details, and research activities of each test cell were identical:

- Construction activities
    - Remove 258 feet of existing concrete pavement
    - Repair existing Class 5 base (if damaged)
    - Install sensors, including vibrating wire strain gauges, quarter-bridge strain gauges, thermocouple trees and maturity loggers
    - Install T2 plates (for thickness verification)
    - Place new concrete layer and conduct tests during paving
    - Fabricate research samples (cylinders/beams) for further lab testing
    - Place new gravel shoulders
- Design details (shown in Figure 2)
    - Panel thickness = 8 inches
    - Panel size = 12 ft W x 15 ft L driving lane
    - Low cementitious mixture with 500 lb/yd^3 of cementitious materials at cell 138 and lower cementitious mixture with 470 lb/yd^3 of cementitious materials at cell 238
    - Shoulders = 2 inch thick shoulder gravel
    - Dowel bars = 1.25 inch diameter epoxy coated steel in standard MnDOT pattern
    - Joints = Single 0.125 inch width saw cut, depth = T/4, unsealed
    - Base: 5.0 in. Class 5 aggregate base
    - Subgrade: Clay loam (A-6)

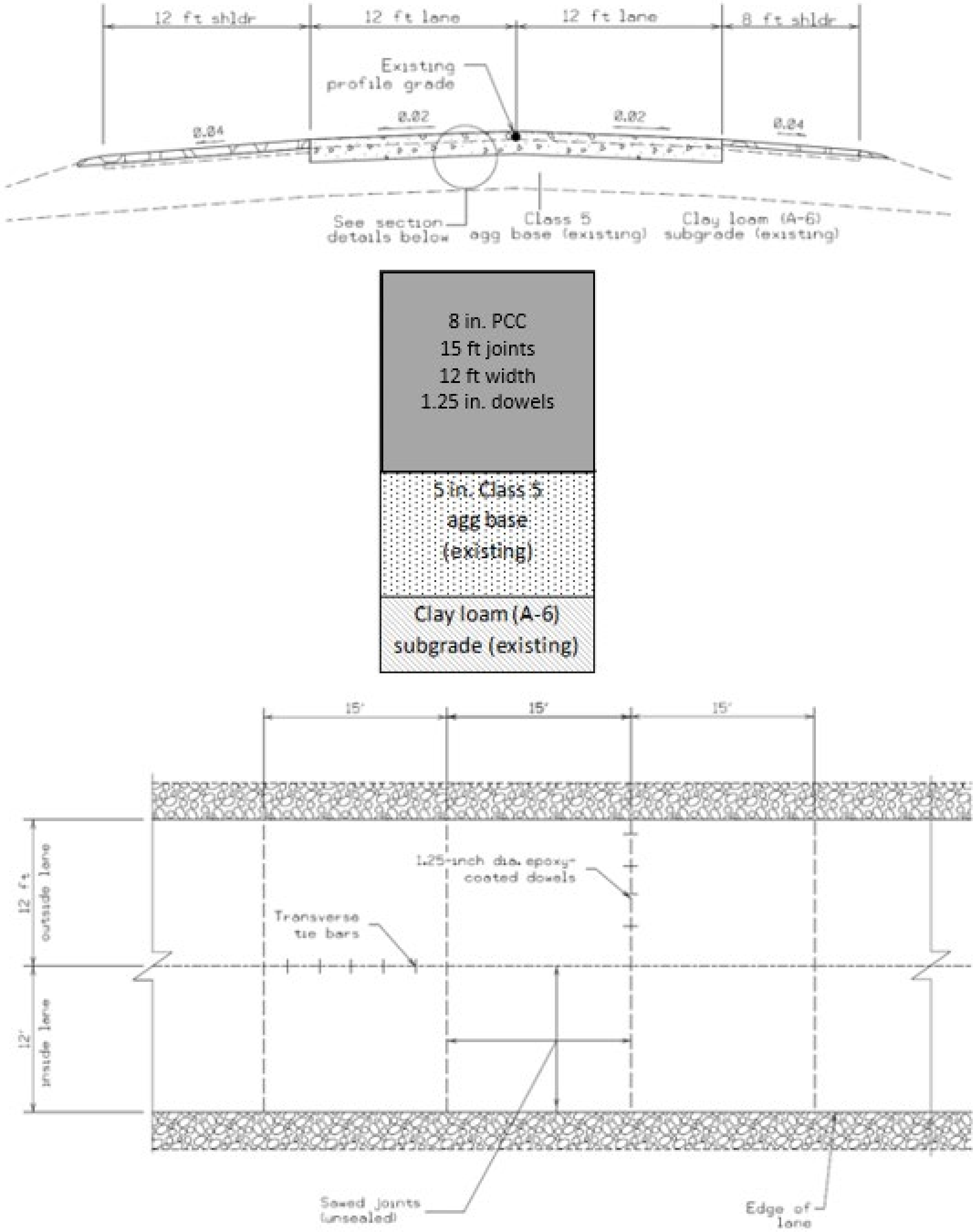

Figure 2- Pavement construction details

MATERIALS

Cementitious Materials

Type I/II Portland cement (ASTM C150) and Class F fly ash (ASTM C618) were used as the cementitious mixtures for all mixtures. A binary system with 25% (by mass) fly ash replacement was used for proportioning the mixtures.

Aggregate

A single source of coarse aggregate, two types of intermediate aggregates, and a natural river sand were used. Table 1 summarizes the physical properties of aggregates.

Table 1- Aggregate properties

Aggregate Type	**Specific Gravity (SSD)**	**Water Absorption (%)**
Coarse	2.73	0.90
Intermediate #1	2.69	1.30
Intermediate #2	2.67	1.50
River Sand	2.63	0.90

Both concrete mixtures were proportioned with an optimized aggregate system, with a weight fraction of 18% coarse aggregate, 33% intermediate #1, 10% intermediate #2, and 39% fine aggregate. The combined aggregate gradations were plotted in a Tarantula curve (Ley et al. 2012), power 45 curve (Kennedy et al. 1994), and Shilstone workability factor chart (Shilstone 1990), as shown in Figure 3.

In the workability factor chart, the workability and coarseness factors of the aggregate system fall within Zone II. The combined aggregate system also met the recommendations of the Tarantula plot.

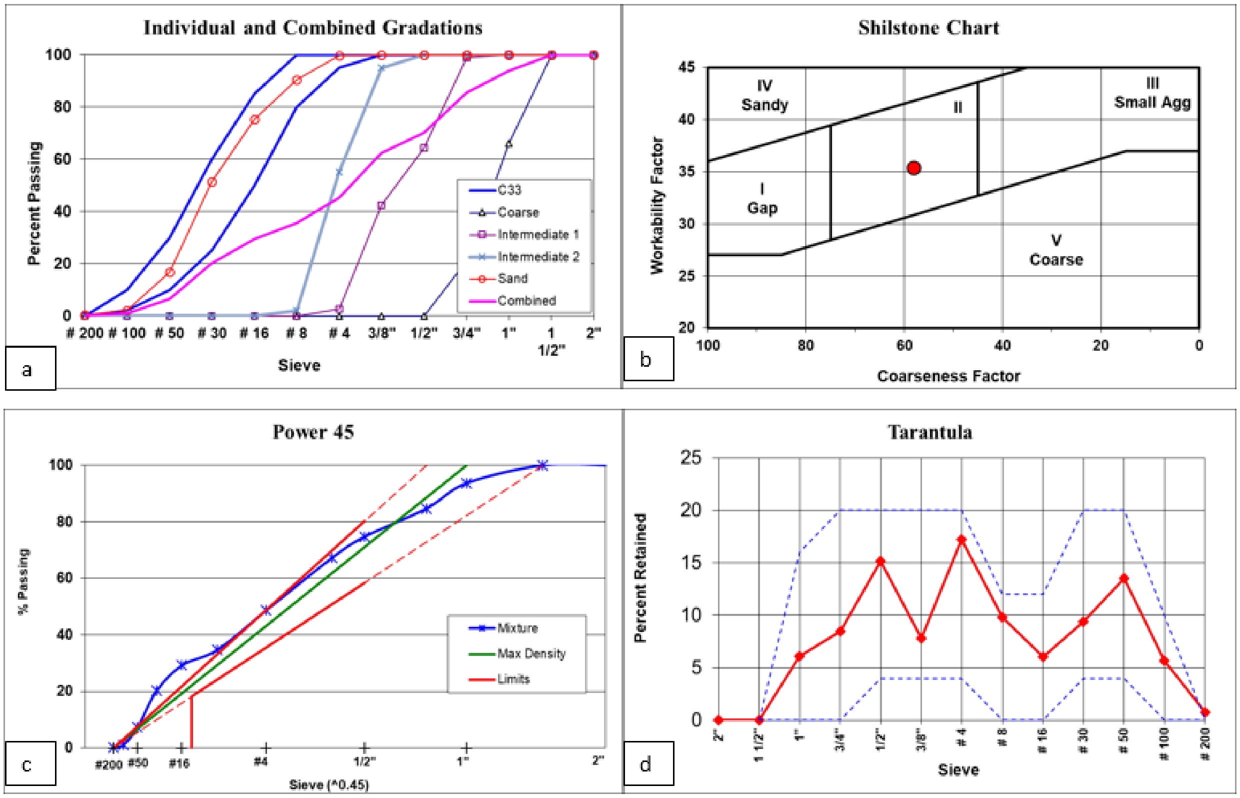

Figure 3- (a) Individual and combined gradations, (b) workability factor chart, (c) power 45 chart, and (d) Tarantula curve

Mixture Proportions

Table 2 offers a summary of the mixture proportions used for casting the pavement at cells 138 and 238, as well as the concrete mixture used for casting the reference pavement at cell 524. The mixtures used for building cells 138 and 238 were proportioned with fixed w/cm of 0.42, while a w/cm of 0.40 was used for the reference concrete used in construction of cell 524. A binary cement with 25% Class F replacement was used for mixtures with low and lower cementitious materials content, compared to 30% fly ash replacement in reference mixture. Air entraining admixture (AEA) and high range water reducing admixture (HRWRA) were used to secure required fresh properties. The percentage voids in aggregate was 27.3% determined based on modified ASTM C 29. Results were incorporated in determining the paste to combined aggregate voids volume ratio (V_{paste}/V_{voids}) using the approach described by Taylor et al. (2015). This approach suggests that V_{paste}/V_{voids} should range between 125 and 175 percent.

Table 2- Concrete mixture proportions

Mix ID	**Unit**	**Type**	**Low Cementitious (Cell 138)**	**Lower Cementitious (Cell 238)**	**Reference (Cell 524)**
Cement	lb/yd^3	Type I/II	375	353	400
Fly Ash	lb/yd^3	Class F	125	117	170
Water	lb/yd^3		210	197	228
w/cm			0.42	0.42	0.40
Coarse Agg.	lb/yd^3		322	328	562
Intermediate #1	lb/yd^3		1,071	1,091	1,015
Intermediate #2	lb/yd^3		589	600	305
Fine Agg.	lb/yd^3		1,235	1,258	1,173
Air Entraining Admixture	oz/cwt		1.0	2.0	
Water Reducing Admixture	oz/cwt	High Range	1.0	1.0	
SCM Dosage	% mass		25	25	30
V_{paste}/V_{voids}	%		146	137	
Unit Weight	lb/ft^3		145.4	146.1	

TEST METHODS

The testing program was divided into three main areas:

- Field tests aimed at assessing the robustness and consistency of the concrete mixtures used for building the cells
- Field/laboratory tests aimed at kinetics of hydration and strength development
- Use of instrumentation, in-situ tests, and inspections aimed at exploring the performance of the pavements over time.

The following field and laboratory tests were conducted:

- VKelly (AASHTO TP 129) (Figure 4)
- Box test (Cook et al. 2014) (Figure 5)
- Semi-adiabatic calorimetry (ASTM C 1753 2015) (Figure 6)
- Maturity, using embedded sensors
- Compressive strength measurement (ASTM C 39)

The following instrumentations and in-situ tests were conducted:

- Ride quality (MnDOT's Light Weight Profiler, ASTM E-950)
- Distress survey (In-situ inspection)

Figure 4- VKelly test setup

Figure 5- Box test showing voids on concrete surface

Figure 6- Calorimetry test setup for measuring the heat of hydration

RESULTS

This section summarizes the relevant data from testing fresh and hardened concrete during the first few days/weeks from casting the cells 138 and 238. In addition, data obtained from embedded sensors and in-situ testing of the pavements, and observations from site inspections are discussed.

Ambient Conditions

The ambient temperature during field testing were in the range of 61.3 to 68.0°F, relative humidity varied from 67 to 87 percent, and wind speed was 3.0 mph.

Testing Fresh Concrete for Workability

Two test methods, V-Kelly and Box Test, were considered to evaluate the workability of the mixtures. Both tests are intended to capture the response of fresh concrete sample to vibration. The V-Kelly test consists of monitoring the rate of penetration of a steel ball of fixed weight into the concrete. An external vibrator is providing energy to the system, which is intended to simulate what happens in front of a paver. The box test on the other hand provides a visual basis for rating the responsiveness of concrete to vibration, where the amount of voids on surface of a vibrated sample is evaluated.

VKelly Test

The VKelly tests indicated that the slump of the mixtures used for cells 138 and 238 were 2.50 and 1.50 in., respectively. The VKelly index of 0.50 in./$s^{0.5}$ obtained for mixture with lower cementitious content was slightly lower than the recommended minimum of 0.60 in./$S^{0.5}$. However, the mixture with low cementitious content used for cell 138 exhibited a VKelly index of 0.88 in./$s^{0.5}$, which was within the recommended range (Taylor et al. 2015). Slight adjustments in WRA dosage were necessary to achieve desirable workability during paving with concrete containing lower cementitious materials content. Observations were in agreement with the V_{paste}/V_{void} data obtained based on mixture proportions presented in Table 2, where values of 146% and 137% were obtained for the concrete with low and lower cementitious materials content, respectively. Observations were in agreement with previous observations of the research team, suggesting 150% as a proper value for V_{paste}/V_{void} while designing paving concrete mixtures.

Box Test

The box test indicated better workability for mixture with low cementitious content. An average visual rating of 1.0 was reported for this mixture, corresponding to less than 10 percent overall surface voids. The visual rating was between 2 and 3 for the concrete with lower cementitious content, indicating 30-50 percent overall surface voids (Cook et al. 2014). No edge slump was observed for the mixtures.

In summary, results obtained for the mixture prepared with low cementitious materials content where within the acceptable ranges and suggest proper workability for construction of cell 138. Potential for workability problems on the other hand was observed for concrete with lower cementitious materials content used for construction of cell 238. This was further verified in following sections of the report.

Testing Fresh Concrete for Kinetics of Hydration

Semi-Adiabatic Calorimetry

The temperature rise data obtained from calorimetry measurements are plotted in Figure 7. Data obtained for both mixtures follow the same pattern, with comparable values during the first 9-10 hours. Even though variations were minor, slightly higher values were observed for the concrete proportioned with low cementitious materials content afterwards. This could be expected given the lower cementitious materials content used in construction of cell 238. However, no abnormalities were observed in terms of delayed setting time and/or rates of increase and decrease in temperature.

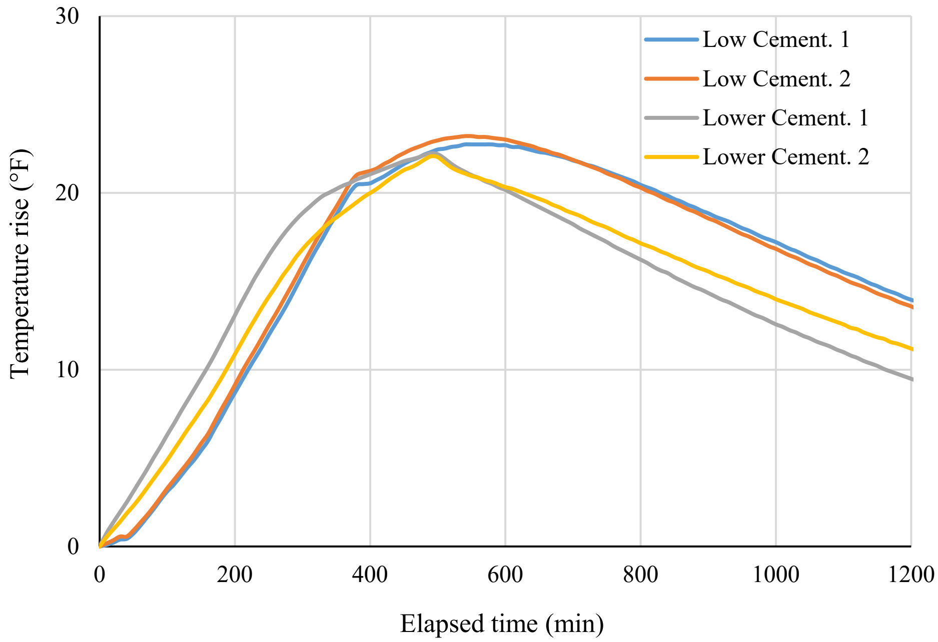

Figure 7- Semi-adiabatic calorimetry temperature rise

Maturity

Figure 8 presents the average maturity data recorded for the mixtures. Similar performance was observed, regardless of the binder content. This was expected given the same binder composition used in both mixtures. Observations were in agreement with the calorimetry results. Similar maturity data obtained for the two investigated mixtures suggest comparable strength development for investigated mixtures, i.e. similar saw-cutting time frame and similar time to potential opening to traffic.

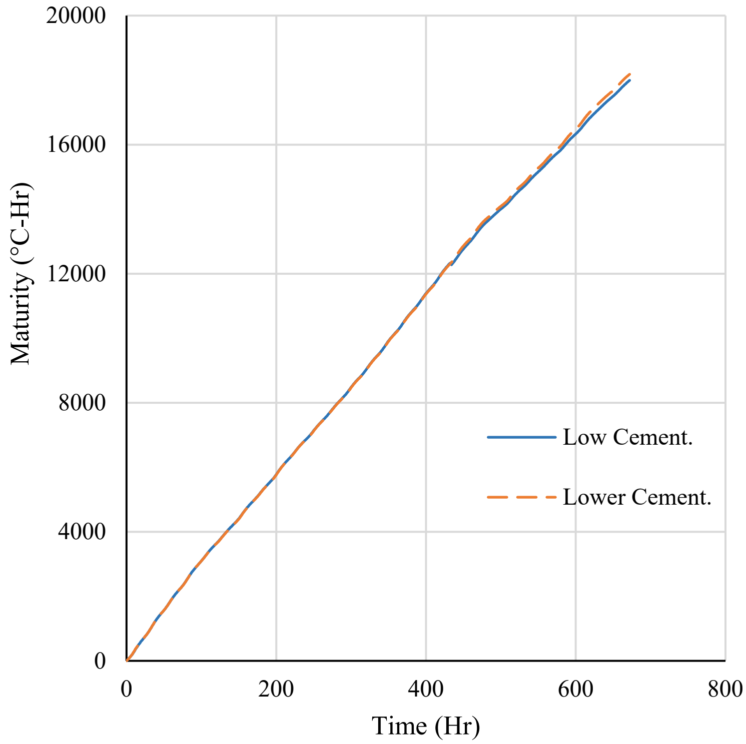

Figure 8- Average maturity data

Testing Hardened Concrete for Strength Development

Compressive Strength

The average compressive strength of the mixtures is presented in Figure 9 for up to 28 days. Comparing the strength development at early age, one can observe that both mixtures exhibited the same compressive strength of 1,750 psi at 48 hours. This was followed by strength values of 2,100±100 psi at 7 days. Comparing the early age compressive strength data confirms the previous observations on kinetics of hydration and concrete maturity, where comparable performance was observed for investigated mixtures.

Given a minimum compressive strength of 3,000 psi is required (MnDOT 2016), results suggest that the mixture prepared with low cementitious materials content can be opened to traffic at about 10 days, compared to 12 days for concrete with lower cementitious materials content. It should be noted that the slightly higher 28-day compressive strength of the concrete with lower cementitious materials content can in part be attributed to the lower air content observed for this concrete (6.5% vs. 8.5%).

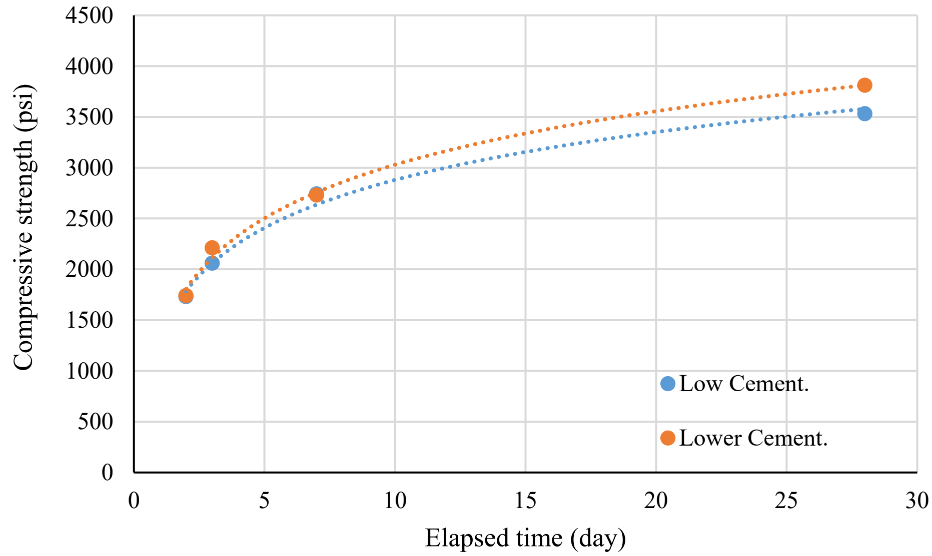

Figure 9- Compressive strength results

Pavement Performance – In-Situ Measurements

In-Situ Static Deformation

Vibrating wire strain gages (VW) embedded at corner and mid-panel areas were used to monitor the total in-situ deformations due to environmental loads. The recorded deformations were caused by a combination of concrete shrinkage, warping due to moisture loss, curling due to temperature gradient within the depth of concrete, and linear deformation of the sensors and the surrounding concrete due to variations in temperature. Table 3 and Figure 10 present the layout and details of the sensor installation.

Table 3- As-built location of sensors installed in mixtures prepared with low and lower cementitious materials content

Cell 138				**Cell 238**			
Sensor #	**Station**	**Offset (ft)**	**Depth (in.)**	**Sensor #**	**Station**	**Offset (ft)**	**Depth (in.)**
VW001	9384.13	11.0	0.8	VW001	9459.00	10.9	0.8
VW002	9384.13	11.0	7.5	VW002	9459.00	10.9	7.5
VW003	9390.16	6.0	0.8	VW003	9464.98	6.0	0.8
VW004	9390.16	6.0	7.5	VW004	9464.98	6.0	7.5

Figure 10- Sensor installation plan for cell 138 (top) and cell 238 (bottom).

Figure 11 presents the strain history recorded during the first week from casting the cells. Time zero readings correspond to the strain values at the time of placing the concrete. For both mixtures, VWSG 1 and VWSG 3 present the deformations close to the surface of the concrete, at corner and mid-panel, respectively, while VWSG 2 and VWSG 4 present the deformations at bottom part of the concrete, at corner and mid-panel, respectively. VWSG 1 and VWSG 2 had transverse orientation, while VWSG 3 and VWSG 4 were oriented longitudinally.

Higher strain values were recorded by the sensors oriented longitudinally. Cyclic patterns could be traced for all sensors, regardless of depth, orientation, and concrete type which was mainly governed by the daily fluctuations in ambient temperature as presented in Figure 12. The sensors located at top parts of the pavement exhibited higher sensitivity to variations in environmental conditions, with a wider range of variation between the recorded minimum and maximum strain values. The highest scatter of about 30 $\mu\varepsilon$ was observed for the first 24 hours. In general, results were comparable for the two investigated cells, indicating similar response of the investigated pavements to environmental conditions at early age.

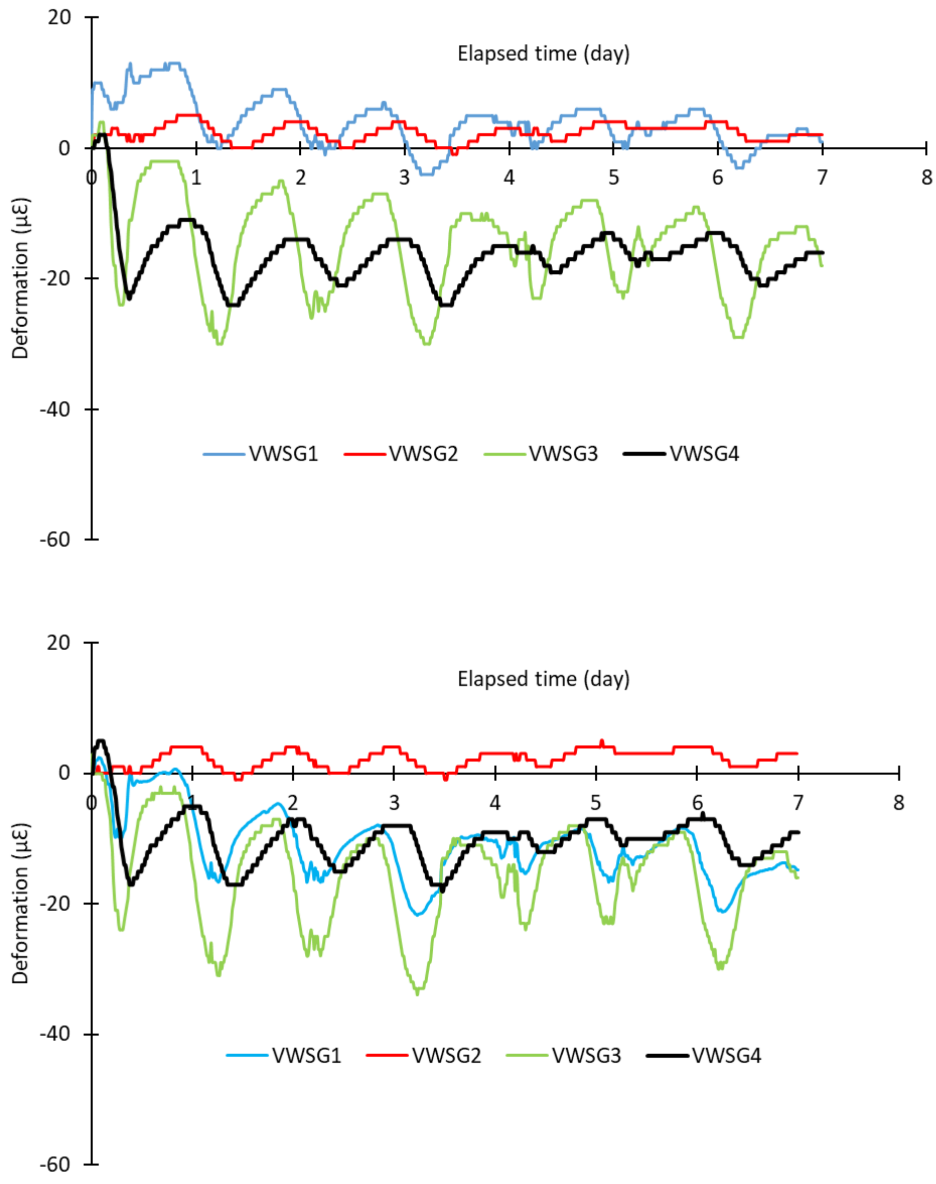

Figure 11- Total in-situ deformation (µɛ) for cell 138 (top) and 238 (bot.)

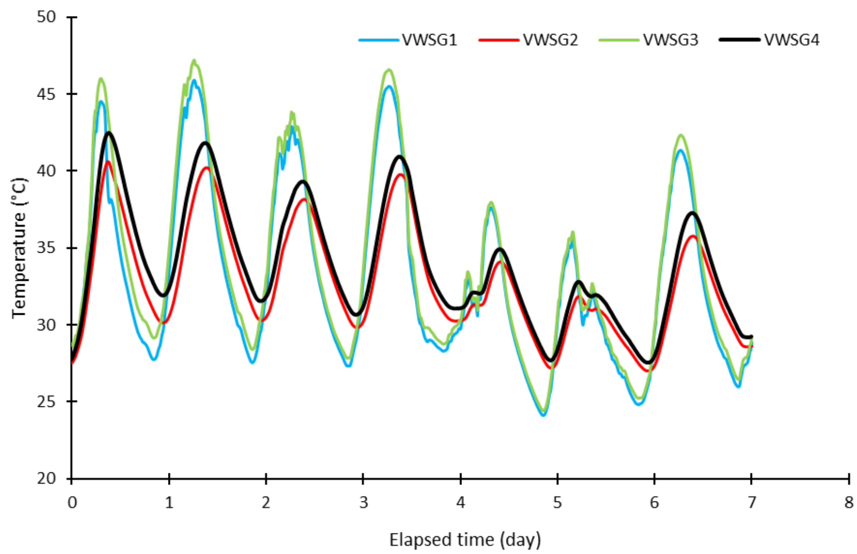

Figure 12- Variation in concrete temperature registered by the VWSGs embedded at cell 238

Evaluating Joint Activation using MIRA test

On September 21st, 2017, a non-destructive test method based on ultrasonic shear-wave tomography was employed to explore the joint activation. The MIRA device (Figure 13) contains 40 dry point contact (DPC) transducers that send and receive low-frequency (55 kHz) shear-wave ultrasonic pulses (Vosoughi and Taylor 2017). The test was repeated 10 times at each joint, and the average results were reported.

Figure 14 presents sample processed data obtained from MIRA test. The left figure is the filter signal and the right figures are obtained by normalizing the transmitted energy across each transducer to transmitted energy of transducer number 6 for determining whether or not cracking occurred at the joint. Normalized values lower than the threshold suggest crack development at examined joints. The obtained data indicated cracking in all joints within cells 138 and 238, while no transverse cracking was observed that could be attributed to delay in saw cutting the joints.

Figure 13- Mira test setup

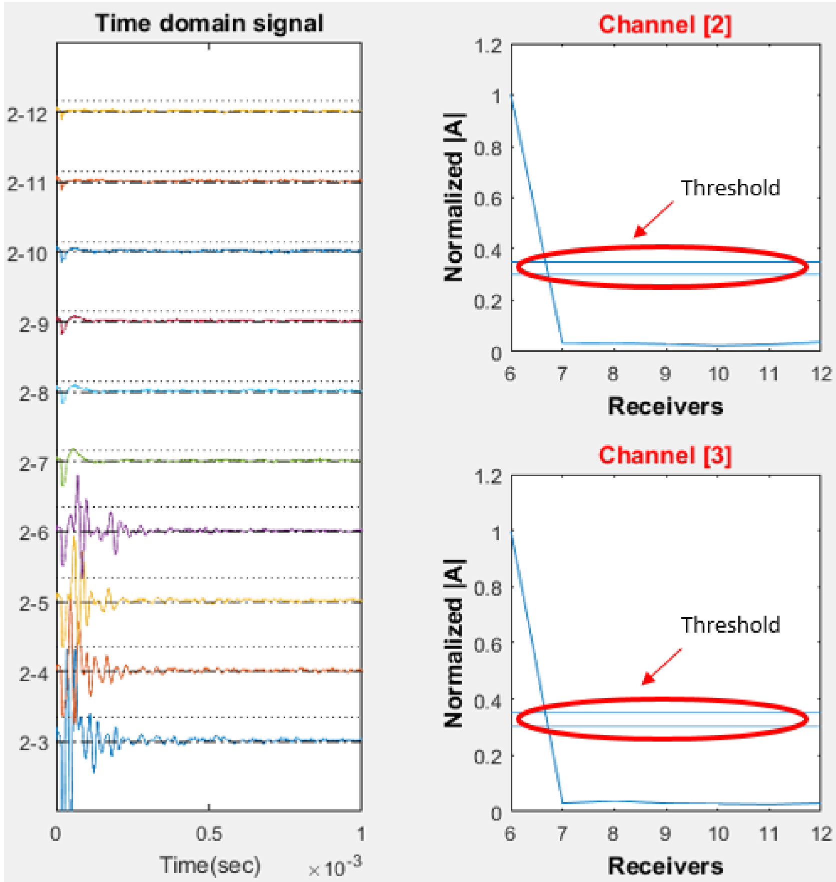

Figure 14- Processed Mira test data

Ride Quality

MnDOT's Lightweight Profiler, conforming to ASTM E-950 requirements (Figure 15) was used for collection of the ride quality data in terms of the International Roughness Index (IRI) according to the following timeline:

Reference Concrete (cell 524): testing was performed on October 26th, 2017, as well as April 25th, June 11th, August 16th, and October 2nd 2018 on both the inside and outside traffic lanes

Low Cement Concrete (cell 138): testing was performed on July 18th, July 20th, July 25th, November 3rd, and November 30th 2017, as well as June 14th, July 9th, and July 26th 2018 on both the inside and outside traffic lanes

Lower Cement Concrete (cell 238): testing was performed on July 18th, July 20th, and July 25th, November 3rd, and November 30th 2017, as well as June 14th, July 9th, and July 26th 2018 on both the inside and outside traffic lanes

Figure 15- MnDOT's Lightweight Profiler

Tables 13-15 summarize the IRI data obtained for the investigated pavements. The reported data are the average of three IRI readings from both the right and left wheel tracks, along with the corresponding Mean Roughness Index (MRI) values. Figure 16 also presents the variation in MRI values over time, for both the inside and outside lanes of the investigated cells during the first year.

The data obtained for the reference cell (cell 524) revealed consistent performance over time, with no significant difference between measurements performed in October 2017 and the ones taken in October 2018. The MRI values obtained for the outside lane of cell 524 were constantly higher than those obtained for the inside lane which is exposed to controlled traffic loading. One should note the difference in thickness of the investigated pavements, where the reference cell is 6.0 in. thick, compared to 8.0-in. thick pavement at cells 138 and 238.

Comparable performance was observed for the cells 138 and 238 for the first year. The MRI values obtained for the outside lane were generally lower than the ones recorded for the inside lane (exposed to traffic) at cell 138. The minimum MRI values were recorded during the first month from construction with values limited to 108 in./mile for both cells. However, an increase in MRI was observed for the measurements taken during the period of November 2017 to July 2018. The increase in MRI was more pronounced for the inside lane which can be due to the exposure to traffic loading. The MRI values obtained for the inside lane ranged from 106 to 139, and from 86 to 110 in./mile for cells 138 and 238, respectively.

It should be noted that a MRI of no more than 65 in./mile is typically recommended by MNDOT. Given the short length of the test cells, such low IRI values are hard to achieve during paving. However, the presented data will only serve as the baseline for comparing the performance of the low cement pavement sections over time. Further data will be available for future annual cell performance reports.

Table 4- Ride quality data for cell 524

Concrete Type	Test Date	Lane	Wheel path	IRI (in./mile)	MRI (in./mile)
Reference; cell 524	10/26/2017	Inside	Left	93.2	99.1
			Right	105.0	
		Outside	Left	101.1	108.1
			Right	115.1	
	03/28/2018	Inside	Left	84.4	89.2
			Right	94.0	
		Outside	Left	93.2	101.2
			Right	109.2	
	04/25/2018	Inside	Left	81.1	85.0
			Right	88.8	
		Outside	Left	85.2	90.6
			Right	96.0	
	06/11/2018	Inside	Left	100.4	110.6
			Right	120.8	
		Outside	Left	109.7	115.9
			Right	122.1	
	08/16/2018	Inside	Left	85.0	89.1
			Right	93.3	
		Outside	Left	94.8	99.2
			Right	103.6	
	10/02/2018	Inside	Left	86.5	95.9
			Right	105.2	
		Outside	Left	96.3	102.3
			Right	108.3	

Table 5- Ride quality data for cell 138

Concrete Type	Test Date	Lane	Wheel path	IRI (in./mile)	MRI (in./mile)
Low cement; cell 138	07/18/2017	Inside	Left	112.7	108.1
			Right	103.5	
		Outside	Left	116.0	102.6
			Right	89.1	
	07/20/2017	Inside	Left	112.5	107.8
			Right	103.1	
		Outside	Left	115.7	102.2
			Right	88.6	
	07/25/2017	Inside	Left	114.5	106.9
			Right	99.2	
		Outside	Left	114.5	101.1
			Right	87.8	
	11/03/2017	Inside	Left	136.35	135.40
			Right	134.64	
		Outside	Left	86.11	88.70
			Right	91.49	
	11/30/2017	Inside	Left	134.13	137.49
			Right	140.98	
		Outside	Left	87.75	90.60
			Right	93.65	
	06/14/2018	Inside	Left	120.45	124.38
			Right	128.37	
		Outside	Left	157.77	139.39
			Right	121.52	
	07/09/2018	Inside	Left	116.84	106.89
			Right	96.75	
		Outside	Left	109.87	110.25
			Right	110.56	
	07/26/2018	Inside	Left	141.80	139.39
			Right	136.79	
		Outside	Left	107.97	100.93
			Right	93.96	

Table 6- Ride quality data for cell 238

Concrete Type	Test Date	Lane	Wheel path	IRI (in./mile)	MRI (in./mile)
Lower cement; cell 238	07/18/2017	Inside	Left	100.8	89.6
			Right	78.5	
		Outside	Left	97.7	104.3
			Right	111.0	
	07/20/2017	Inside	Left	100.8	89.7
			Right	78.6	
		Outside	Left	100.8	105.0
			Right	109.2	
	07/25/2017	Inside	Left	98.2	87.1
			Right	75.9	
		Outside	Left	100.8	104.5
			Right	108.2	
	11/03/2017	Inside	Left	93.52	86.80
			Right	80.09	
		Outside	Left	124.63	133.50
			Right	142.12	
	11/30/2017	Inside	Left	118.48	110.44
			Right	102.45	
		Outside	Left	125.01	132.61
			Right	140.47	
	06/14/2018	Inside	Left	116.77	110.25
			Right	103.66	
		Outside	Left	90.54	94.41
			Right	98.71	
	07/09/2018	Inside	Left	93.58	87.88
			Right	82.37	
		Outside	Left	114.30	115.13
			Right	115.57	
	07/26/2018	Inside	Left	104.42	94.85
			Right	85.22	
		Outside	Left	129.63	133.69
			Right	137.55	

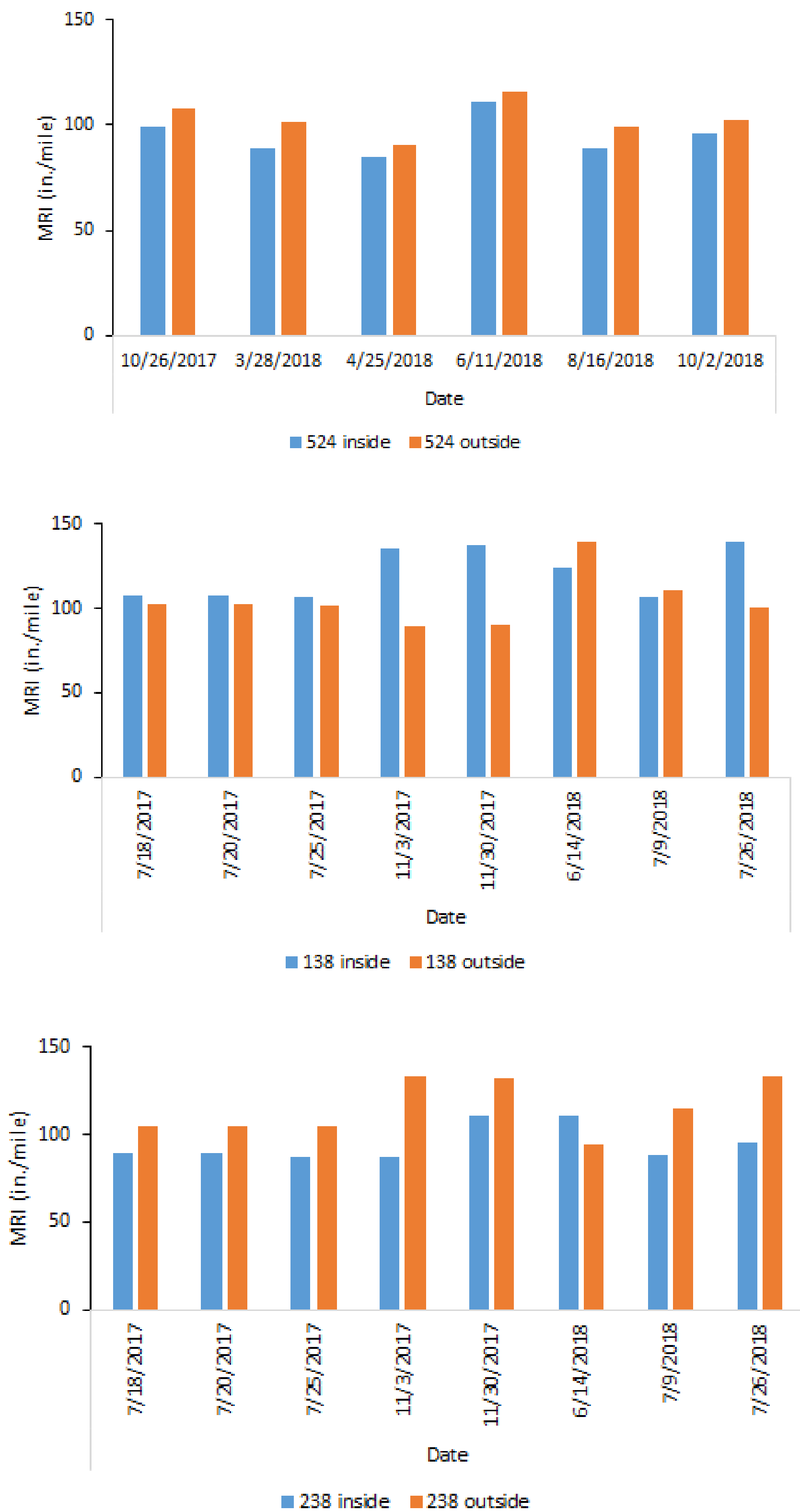

Figure 16- Variation in MRI (in./mile) values as a function of time

In-Situ Inspection

In-situ inspection of the cells after over one year of exposure to environmental conditions and traffic loading was conducted in November 2018. Figure 17 presents examples of typical surface quality at cell 138. Observations indicated proper quality of the pavement surfaces at cell 138, where minimal issues were observed with the surface texture. This verifies the proper finishing in light of adequate workability of the mixture with low cementitious materials content. A closer look at the surfaces also reveals uniform texture of the pavement surfaces at cell 138 as shown in Figure 18. Moreover, both the transverse and the longitudinal joints were in good shape and no signs of raveling and/or joint damage and staining could be detected. Examples of typical quality of longitudinal and traverse joints after over one year of service are shown in Figure 19.

In general paved surfaces at cell 238 exhibited acceptable quality as can be seen in Figure 20. Finishing problems were occasionally observed at pavement surfaces in cell 238 as shown in Figure 21. This is believed to be due to the lower workability of the mixtures with lower cementitious materials content as discussed earlier in this report.

Even though the mixture prepared with lower cementitious materials content developed same maturity and early age compressive strength data to those of the mixture used in cell 138, occasional raveling could be detected at longitudinal joints at cell 238. This could be due to the reduced cohesion of the mixture and the reduced coverage of coarse aggregate with paste. Finishing problems may have also contributed to these observations. Figure 22 presents examples of typical surface quality and the observed finishing problems at cell 238.

Figure 17- Examples of typical pavement surfaces at cell 138

Figure 18- Examples of typical pavement texture at wheel path of cell 138

Figure 19- Example of typical condition of longitudinal joints (top) and transverse joints (bot.) at cell 138

Figure 20- Examples of typical pavement surfaces at cell 238, outside lane (top), inside lane (bot.)

Figure 21- Examples of typical pavement surfaces at cell 138

Figure 22- Typical condition of longitudinal joints (top) and occasional raveling (bot.) at cell 138

KEY FINDINGS

Based on the presented results, the following findings are developed:

- The mixture prepared with low cementitious materials content of 500 lb/yd^{3}exhibited acceptable workability based on VKelly and Box test results. Slight workability problems were observed for the mixture with lower cementitious materials content of 470 lb/yd^3.
- The investigated mixtures exhibited similar 2- and 7-day compressive strength of 1,750 psi and 2,100±100 psi, respectively. The comparable early age strength data were in line with the data obtained from investigating the heat of hydration and maturity of the mixtures. Both mixtures developed compressive strength of 3,000 psi before 14 days, which is MnDOT's strength requirement for opening to traffic.
- MIRA measurements indicated cracking in all joints along the experimental section regardless of the cementitious materials content.
- Comparable ride quality data was observed for the investigated cells.
- The early age in-situ deformations were limited to 30 $\mu\varepsilon$ for both mixtures, where variation in deformations and strains were dominated by the daily changes in ambient temperature regardless of the concrete mixture type.
- In-situ inspection verifies proper finishing and surface quality of pavement at cell 138, along with high quality at saw cut joints. Finishing problems and raveling at longitudinal joints were more common at cell 238, indicating that given the incorporated aggregate combinations, concerns may raise while the total cementitious materials content is reduced to 470 lb/yd^3.
- Results obtained through this study suggest that the V_{paste}/V_{void} ratio of 146 obtained for the mixture with low cementitious materials content yields proper workability and early age performance of the paving mixture and can be considered as the lower limit for mixture proportioning purposes. However, the V_{paste}/V_{void} ratio of 137 obtained for the mixture with lower cementitious materials was borderline too low.

REFERENCES

American Association of State Highway and Transportation Officials (AASHTO). 2017. *Standard Method of Vibrating Kelly Ball (VKelly) Penetration in Fresh Portland Cement Concrete*. AASHTO TP 129. AASHTO, Washington, DC.

ASTM C29 / C29M-17a, *Standard Test Method for Bulk Density ("Unit Weight") and Voids in Aggregate*, ASTM International, West Conshohocken, PA, 2017

ASTM C39 / C39M-18, *Standard Test Method for Compressive Strength of Cylindrical Concrete Specimens*, ASTM International, West Conshohocken, PA, 2018

ASTM C150 / C150M-17, Standard Specification for Portland Cement, ASTM International, West Conshohocken, PA, 2017

ASTM C618-17a, *Standard Specification for Coal Fly Ash and Raw or Calcined Natural Pozzolan for Use in Concrete*, ASTM International, West Conshohocken, PA, 2017

ASTM C1753 / C1753M-15e1, *Standard Practice for Evaluating Early Hydration of Hydraulic Cementitious Mixtures Using Thermal Measurements*, ASTM International, West Conshohocken, PA, 2015

ASTM E950-98, *Standard Test Method for Measuring the Longitudinal Profile of Traveled Surfaces with an Accelerometer Established Inertial Profiling Reference*, ASTM International, West Conshohocken, PA, 1998

Cook, D., Ghaeezadah, A., and Ley, T. 2014. *A Workability Test for Slip Formed Concrete Pavements*. Construction and Building Materials, Vol. 68, pp. 376–383.

Kennedy, T., Huber, G., Harrigan, E., Cominsky, R., Hughes, C., Quintus, H., and Moulthrop. J. 1994. *Superior Performing Asphalt Pavements (Superpave): The Product of SHRP Asphalt Research Program*. Strategic Highway Research Program, Washington, DC.

Ley, T., Cook, D., and Fick. G. 2012. *Concrete Pavement Mixture Design and Analysis (MDA): Effect of Aggregate Systems on Concrete Properties*, National Concrete Pavement Technology Center, Ames, IA.

Minnesota Department of Transportation (MnDOT). 2016. *Standard Specifications for Construction. Section 2301: Concrete Pavement*. MnDOT, St. Paul, MN. https://www.dot.state.mn.us/materials/concretedocs/Section_3_2301_Specifications.pdf

Shilstone, J. M. 1990. *Concrete Mixture Optimization*. Concrete International, American Concrete Institute (ACI), 12(6): 33–39.

Taylor, P., Wang, X., and Wang, X. 2015. *Concrete Pavement Mixture Design and Analysis (MDA): Development and Evaluation of Vibrating Kelly Ball Test (VKelly Test) for the Workability of Concrete*. National Concrete Pavement Technology Center, Ames, IA.

Vosoughi, P., Taylor, P., *Impacts of Internal Curing on the Performance of Concrete Materials in the Laboratory and the Field*. National Concrete Pavement Technology Center, Ames, IA.